Molecular Crystals and Liquid Crystals Science and Technology. Section A. Molecular Crystals and Liquid Crystals

Publication details, including instructions for authors and subscription information:
http://www.tandfonline.com/loi/gmcl19

Spectroscopic Studies on BDNT Having a Property of One-Step Two-Electron Oxidation: $BDNT^{0}$, $BDNT^{1+}$, and $BDNT^{2+}$

Kyuya Yakushi [a], Jian Dong [a], Mikio Uruichi [a] & Yoshiro Yamashita [a]

[a] Institute for Molecular Science and the Graduate University for Advanced Studies, Myodaiji, Okazaki, 444, Japan

Version of record first published: 24 Sep 2006.

To cite this article: Kyuya Yakushi , Jian Dong , Mikio Uruichi & Yoshiro Yamashita (1996): Spectroscopic Studies on BDNT Having a Property of One-Step Two-Electron Oxidation: $BDNT^{0}$, $BDNT^{1+}$, and $BDNT^{2+}$, Molecular Crystals and Liquid Crystals Science and Technology. Section A. Molecular Crystals and Liquid Crystals, 284:1, 223-234

To link to this article: http://dx.doi.org/10.1080/10587259608037925

Mol. Cryst. Liq. Cryst., 1996, Vol. 284, pp. 223–234
Reprints available directly from the publisher
Photocopying permitted by license only

SPECTROSCOPIC STUDIES ON BDNT HAVING A PROPERTY OF ONE-STEP TWO-ELECTRON OXIDATION: $BDNT^{0}$, $BDNT^{1+}$, AND $BDNT^{2+}$

KYUYA YAKUSHI, JIAN DONG, MIKIO URUICHI, and
YOSHIRO YAMASHITA
Institute for Molecular Science and the Graduate University for Advanced Studies, Myodaiji, Okazaki, 444 Japan

Abstract The neutral molecule, monocation, and dication of BDNT, which shows a one-step two-electron oxidation property, were characterized by a spectroscopic method. The extreme closeness of the first and second oxidation potentials is ascribable to the large structural change from $BDNT^{1+}$ to $BDNT^{2+}$. The on-site Coulomb energy U and transfer integral t of monoclinic BDNT-PF_6 were estimated to be 0.8 eV and 0.13 eV, respectively. The coupling constants of the vibronic band were estimated by the least-squares fitting of the dimer-model function to the observed conductivity spectrum. These coupling constants shows that $BDNT^{1+}$ is rather rigid compared with TTF, TCNQ, or Chloranil.

INTRODUCTION

BDNT (4,9-bis(1,3-benzodithiol-2-ylidene)-4,9-dihyronaphtho[2,3-c][1,2,5] thiadiazole) **1** has a peculiar electrochemical property that the first and second oxidation potentials are not resolved. From the analysis of the width of the oxidation wave, the difference between the first and second oxidation potentials (ΔE) is estimated to be 0.024 eV.[1]

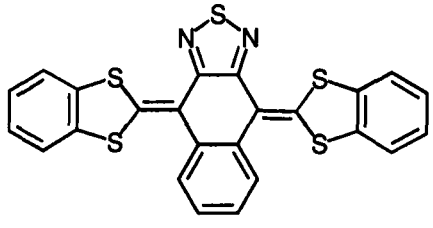

BDNT

1

This molecule has a steric hindrance between S of the dithiole ring and the *peri*-hydrogen of the benzene ring and a strong attraction between S of dithiole and N of the thiadiazole ring.[2] Due to this attractive force, the benzodithiole rings are not twisted against the naphthothiadiazole but are bent by 22° keeping a π-conjugation with the naphthothiadiazole. Owing to the extreme closeness of the first and second oxidation potentials, stable charge-transfer salts of monocation and dication are isolated. Few molecules give such stable monovalent and divalent salts. This electrochemical property is reflected on the disproportionation in an acetonitrile solution of BDNT-PF_6, where $BDNT^{1+}$ is disproportionated into $BDNT^0$ and $BDNT^{2+}$.[3] Our interest in this molecule is to investigate the possibility of the *negative-U state*[4] or disproportionated state in solid state.

CHARACTERIZATION OF $BDNT^0$, $BDNT^{1+}$, AND $BDNT^{2+}$

Electronic spectra

Figure 1 shows the comparison of the solution spectra of $BDNT^0$, $BDNT^{1+}$, and $BDNT^{2+}$. Since $BDNT^{1+}$ sometimes shows a disproportionation reaction such as $2BDNT^{1+} \rightarrow BDNT^0 + BDNT^{2+}$, these solution spectra were carefully identified taking account of the chemical equilibrium in solution.[3] The lowest absorption band of $BDNT^{1+}$ appears at 8.08×10^3 cm^{-1}. This absorption band becomes the key band of $BDNT^{1+}$, since no electronic transition appears in $BDNT^0$ and $BDNT^{2+}$ in this spectral region.

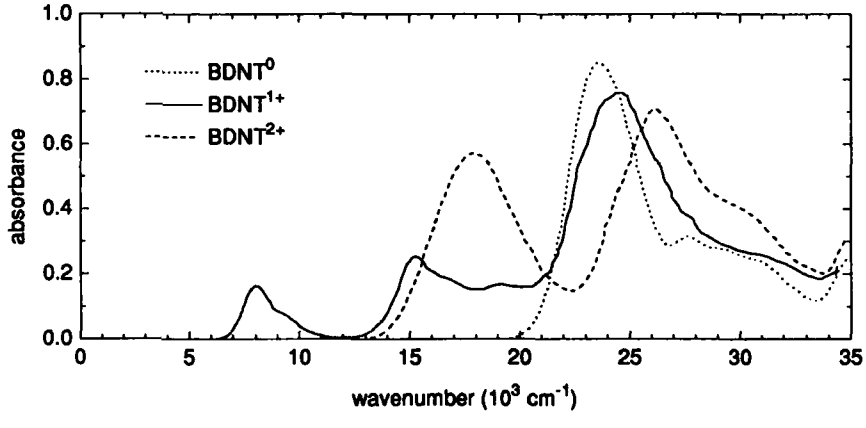

FIGURE 1 Solution spectra of $BDNT^0$, $BDNT^{1+}$, and $BDNT^{2+}$.

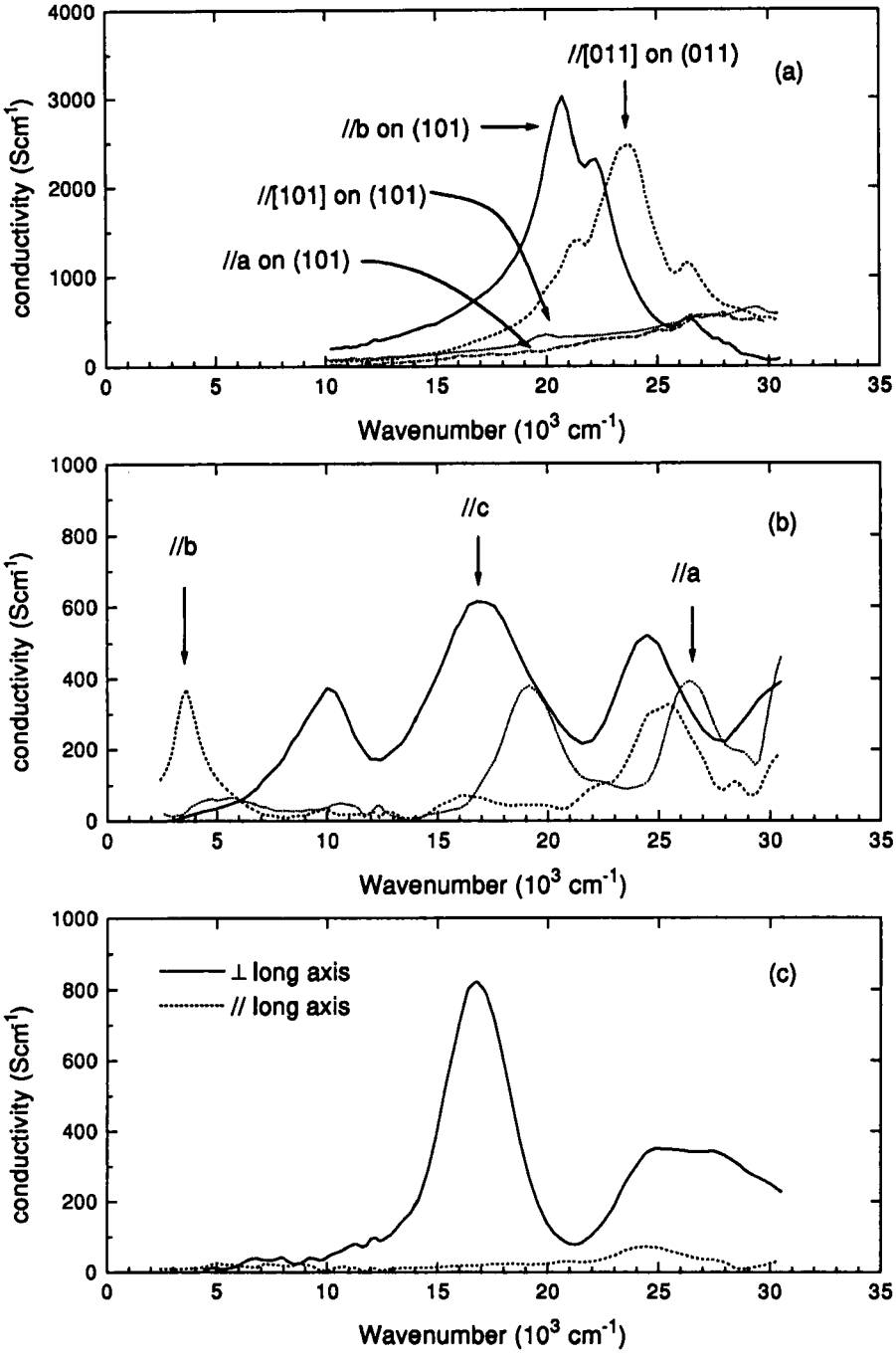

FIGURE 2 Polarized spectra of the single crystals of (a) BDNT, (b) *m*-BDNT-PF_6, and (c) BDNT-$(PF_6)_2$.

The conductivity spectra obtained from the Kramers-Kronig transformation of the reflection spectra were displayed in Fig. 2. In the solid spectrum of $BDNT^0$, a large splitting was observed between the two polarizations, //*b* on (101) and //[011] on (011). This is not due to the two different electronic transitions nor the Davidov splitting. This splitting was qualitatively explained in terms of the directional dispersion theory.[3] It was concluded from this analysis that there were three electronic transitions, a weak transition at 20×10^3 cm^{-1} polarized in the short molecular axis, and strong and weak transitions at 20.6×10^3 cm^{-1} and 26.3×10^3 cm^{-1} polarized in the long molecular axis. The key absorption band of $BDNT^{1+}$ was observed in the spectrum of *m*-BDNT-PF_6 (monoclinic form), which means that the disproportionation or mixed valence state between $BDNT^0$ and $BDNT^{2+}$ does not occur in this charge-transfer salt.

Vibrational spectra

From the comparison with the single crystal data, most of the strong bands in the powdered samples of BDNT, *m*-BDNT-PF_6, and BDNT-$(PF_6)_2$ are polarized in the long molecular axis.[3] In the spectrum of *m*-BDNT-PF_6, several vibronic bands are observed already at room temperature. These vibronic bands showed a remarkable enhancement at low temperature below 150 K. Probably a fluctuation of the dimeric lattice distortion exists already at room temperature.

In TTF and BEDT-TTF, the Raman active stretching modes of C=C , which connects the dithiole rings, are sensitive to the valence, and their frequency shifts are used to estimate the valence of the molecules. The Raman active modes of BEDT-TTF and TTF are listed in Table 1, along with the bond lengths of the central C=C bond. There is a good correspondence between the resonance frequencies and bond lengths: the longer the bond length, the lower the frequency. The C=C stretching mode of $BDNT^0$ was assigned to the 1509 cm^{-1} band taking account of the bond length of $BDNT^0$.[3] We tentatively assigned the same vibrational mode of $BDNT^{1+}$ to the 1487 cm^{-1} band and the corresponding mode of $BDNT^{2+}$ to 1435 cm^{-1}. The Raman active mode has been assigned to 1509 cm^{-1} for $BDNT^0$, 1478 cm^{-1} for $BDNT^{1+}$, and 1427 cm^{-1} for $BDNT^{2+}$.[5]

TABLE I Bond lengths of C=C and the resonance frequencies of the stretching modes of BDNT, BEDT-TTF, and TTF.

	bond length (Å)	frequency (cm^{-1})		bond length (Å)	frequency (cm^{-1})		bond length (Å)	frequency (cm^{-1})
$BDNT^0$	1.37	1509 IR	BEDT-	1.32[6]		TTF^0	1.35[8]	
		1509 Ra[5]	TTF^0		1552 Ra[7]			1518 Ra[9]
$BDNT^{1+}$	1.38	1487 IR	BEDT-	1.39[10]		TTF^{1+}	1.40[12]	
		1478 Ra[5]	TTF^{1+}		1455 Ra[11]			1420 Ra[9]
$BDNT^{2+}$	1.44	1435 IR	BEDT-	1.44[8]	–	TTF^{2+}	–	–
	-1.5	1427 Ra[5]	TTF^{2+}					

Molecular geometry of $BDNT^0$, $BDNT^{1+}$, and $BDNT^{2+}$

Table 2 shows the lattice parameters of BDNT and its (1:1) and (1:2) charge-transfer salts. Both $BDNT^0$ and $BDNT^{1+}$ are butterfly-shaped and their geometries are quite similar to each other. Due to this molecular shape, BDNT and $BDNT^{1+}$ are stacked and make a molecular column structure. Usually the C=C bond length is sensitive to the valence and elongates upon oxidation, but the corresponding bond length of $BDNT^{1+}$ does not change much as shown in Table 1. The geometrical change of the naphthothiadiazole ring is larger rather than that of C=C and dithiole ring.

TABLE II Lattice parameters of BDNT and its charge-transfer salts

	BDNT	*m*-BDNT-PF_6	*m*-BDNT-ClO_4	*m*-BDNT-SbF_6	BDNT-$(ClO_4)_2$-CH_2Cl_2	BDNT-$(SbF_6)_2$
space group	Pnma	$P2_1/a$	$P2_1/a$	$P2_1/c$	P1	P1
a (Å)	8.136(1)	20.755(7)	19.534(8)	17.472(4)	14.087(1)	8.430(5)
b (Å)	18.796(3)	7.216(1)	7.202(2)	7.239(7)	14.587(1)	14.294(6)
c (Å)	13.540(1)	17.095(5)	16.094(7)	21.108(3)	7.535(1)	14.35(2)
α (°)	90	90	90	90	92.89(1)	112.76(7)
β (°)	90	107.97(1)	93.30(2)	110.13(1)	97.47(1)	94.77(7)
γ (°)	90	90	90	90	73.44(1)	94.75(4)
V ($Å^3$)	2070.4(4)	2436(1)	2264(1)	2506(1)	1471.4(2)	1576(2)
Z	4	4	4	4	2	2

On the other hand, the geometry of $BDNT^{2+}$ is quite different from $BDNT^{0}$ and $BDNT^{1+}$. Interestingly, two different geometries were found in $BDNT^{2+}$: One of the dithiole rings is bent by 19° and another is twisted by 46° against the naphthothiadiazole ring in BDNT-$(ClO_4)_2$-CH_2Cl_2, and both the dithiole rings are twisted by 45° against the naphthothiadiazole ring in BDNT-$(SbF_6)_2$. The crystal structure of BDNT-$(PF_6)_2$ is not known due to the quality of the crystal. We suppose, however, that it has a similar structure as BDNT-$(SbF_6)_2$, since PF_6^- has the same shape and nearly the same size as SbF_6^-. Due to these non-butterfly shapes, the packing motif is entirely different from the stacked column structure. The molecular geometries of these compounds viewed along the short molecular axis are shown in Fig. 3. A good correspondence of the electronic spectra of solid and solution shown in Figs. 1 and 2 suggests that the $BDNT^{2+}$ has a twisted structure in solution as well. This means that the structural change from $BDNT^{1+}$ to $BDNT^{2+}$ is much larger than that from $BDNT^{0}$ to $BDNT^{1+}$.

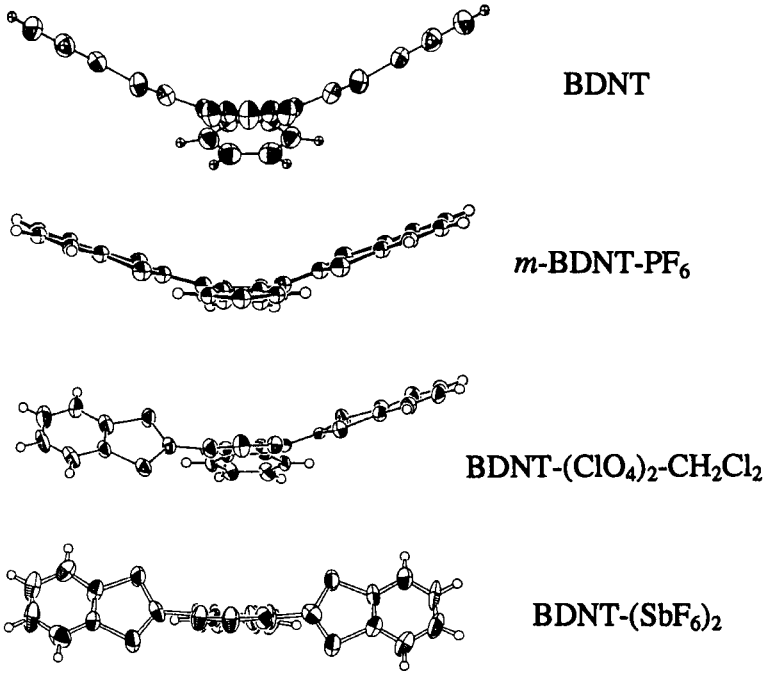

FIGURE 3 Molecular geometry of $BDNT^{0}$, $BDNT^{1+}$, and $BDNT^{2+}$.

This structural dependence upon valence is different from that of BEDT-TTF, where the C=C bond lengthens almost linearly from BEDT-TTF^{0} to BEDT-TTF^{2+} as shown in Table 1. The non-linear structural change of BDNT is related to the bent and rather rigid structure of BDNT resulted from the balance of the S···N attractive force and S···H repulsive force. This rigid structure pushes up the first oxidation potential. The twisting of the benzodithiole rings releases the above attractive and repulsive forces and makes the geometry more flexible. This large geometrical relaxation pulls down the second oxidation potential. Consequently, this non-linear structural change is the origin of the extreme closeness of the first and second oxidation potential.

INVESTIGATION OF *m*-BDNT-PF_6

In solid state the molecule is not so flexible as in solution. We examined the on-site Coulomb energy and the coupling constants of the vibranic modes of *m*-BDNT-PF_6. The crystal of *m*-BDNT-PF_6 is a thick plate elongated along the *b*-axis with a well-developed (001) face. The molecules are stacked along the *b*-axis, and the neighboring molecules in the stack are related to each other by the screw axis running along the *b*-axis. Due to this screw-axis symmetry, the molecules are connected by a single transfer integral along the *b*-axis, although the repeating unit is two molecules.

Analysis of the charge-transfer band

The charge-transfer band is observed at 3500 cm^{-1}, which is quite low among the usual (1:1) charge-transfer salts. Since the repeating unit of BDNT along the *b*-axis is two molecules and one BDNT molecule provides one electron, a band gap is open at the Fermi level due to the periodic electrostatic potential of PF_6^-. However, this bandgap is not mainly determined by the periodic potential of PF_6^-, since a very similar spectrum was observed in the orthorhombic form (*o*-BDNT-PF_6) in which the repeating unit of BDNT is a single molecule. Thus the excitation energy of this 3500 cm^{-1} band is determined by the on-site Coulomb energy on the BDNT molecule like an ordinary organic charge-transfer salt. The small spin excitation energy (500 cm^{-1}) estimated by the temperature dependence of the ESR experiment confirms this conclusion as well.

From the integration of the $\sigma(\omega)$ spectrum, the oscillator strength of the charge-transfer band was estimated to be 0.16_7 at room temperature. The absorption edge is defined by the position at which the conductivity $\sigma(\omega)$ has half of the peak value. The room-temperature value is 3000 cm^{-1} (0.37 eV). Since this material is a correlated electron system, the one-dimensional Hubbard model is applicable to this compound. We estimated the Hubbard parameters U and t using the exact solutions of the excitation energy[13] and oscillator strength[14] for the one-dimensional Hubbard model of a half-filled case.[15] The on-site Coulomb energy U and the transfer integral t were estimated as 0.8 eV and 0.1_3 eV, respectively. The parameters (U and t) which were estimated using the same way in other one-dimensional organic conductors are (1.2 and 0.2)[16] for Rb-TCNQ-II, (1.1 and 0.1_4)[17] for BEDT-TTF-($AuCl_2Br_2$), and (0.5 and 0.1_5)[18] for TTF-TTP-I_3. U of BDNT is considerably small but is not so small as expected from the electrochemical experiment. This is natural because the large geometrical change is not accessible in solid state in contrast to the case in solution, but U is still considerably small probably due to the large size of the molecule.

Analysis of the vibronic bands

A remarkable enhancement of several vibronic bands was observed in the reflection spectrum polarized along the b-axis as shown in the top panel of Fig. 4. The conductivity spectrum in the infrared region is drawn in the bottom panel. It is well known that the vibronic mode (or emv coupled mode) is very sensitive to the lattice dimerization, and has been used as a probe of a small lattice dimerization.[19] This observation strongly indicates the lattice dimerization at low temperature.

Although many theoretical and experimental studies have been reported on the vibronic modes of organic CT salts, the coupling constants of vibronic modes have been experimentally determined only for a few molecules. We analyzed the infrared spectrum at 15 K using the following equations.[20]

$$\sigma(\omega) = \frac{\omega}{i}\frac{N_d e^2 a^2}{4}\frac{\chi(\omega)\chi(0)}{\chi(0) - \chi(\omega)D(\omega)}$$

$$D(\omega) = \sum_{\alpha}\frac{\lambda_{\alpha}\omega_{\alpha}^2}{\omega_{\alpha}^2 - \omega^2 - i\omega\gamma_{\alpha}}$$

where the electric susceptibility $\chi(\omega)$ is defined by

$$\chi(\omega) = \frac{2\omega_{CT}|\langle CT|\delta n|G\rangle|^2}{\omega_{CT}^2 - \omega^2 - i\omega\gamma_{CT}}$$

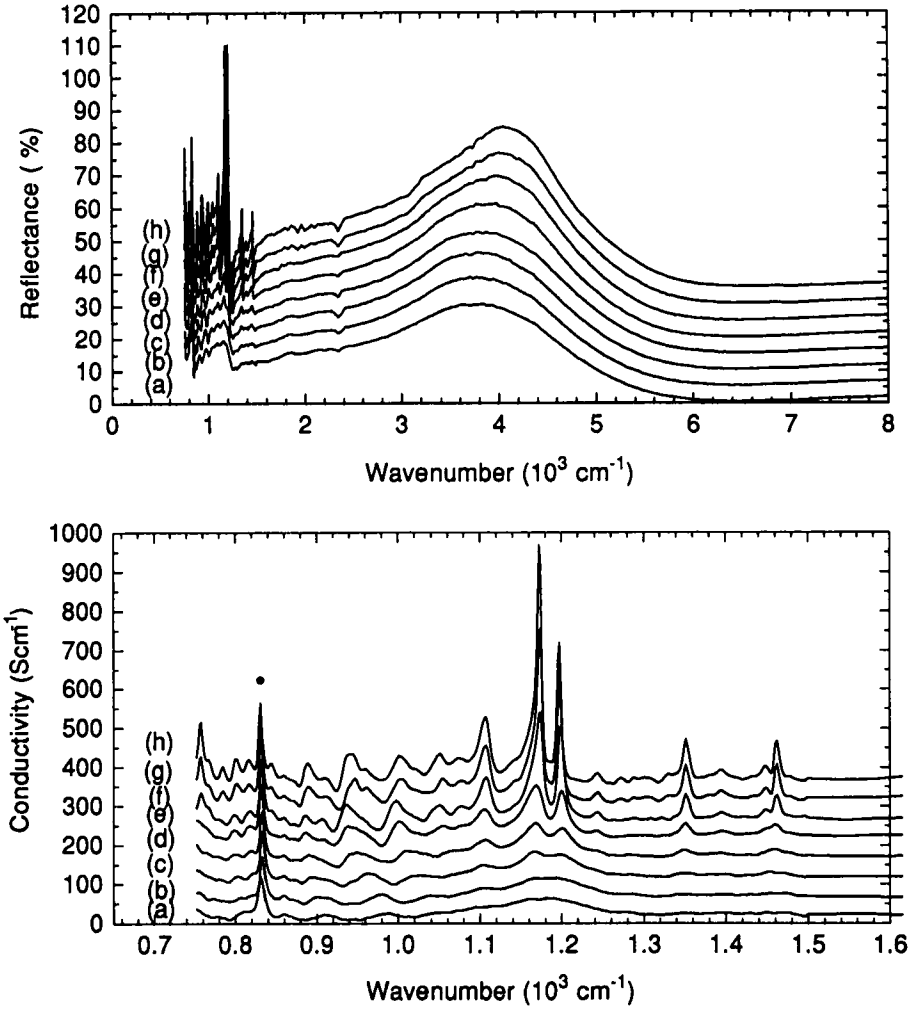

FIGURE 4 Temperature dependence of the reflection and conductivity spectra of *m*-BDNT-PF_6. (a) 297 K, (b) 253 K, (c) 203 K, (d) 154 K, (e) 104 K, (f) 75 K, (g) 46 K, and (h) 15 K. An asterisk denotes the vibrational band of PF_6^-.

ω_{CT} is the frequency of the charge-transfer transition, N_d the number of dimers in a unit volume, a the intermolecular distance. The set of parameters (λ_α, ω_α, γ_α) describes the feature of the vibronic mode: λ_α is the dimensionless coupling constant, ω_α unperturbed frequency, γ_α line width or damping constant. The dimer model is known to be a good approximation for determining the coupling constants of the dimerized chain system.[21] The observed conductivity spectrum in the region of 800 - 8000 cm^{-1} was reproduced very well by the least-squares fitting, and the best-fit parameters are ω_{CT}= 3495 cm^{-1}, $2|\langle CT|\delta n|G\rangle|^2 = 1.58$, γ_{CT}= 1009 cm^{-1}, and the parameters listed in Table 3. The unperturbed frequency ω_α shown in the second column, which was estimated by this analysis shows a good agreement with the Raman line shown in the third column. This good agreement guarantees the reliability of these coupling constants.

TABLE III Parameters for the vibronic modes at 15 K

Ω_α (cm^{-1})[a]	ω_α (cm^{-1})[b]	ω_α (cm^{-1})[c]	λ_α[d]	γ_α (cm^{-1})[e]	g_α (meV)[f]
1462	1476	1478	0.026	20	36
1352	1367	1369	0.027	15	35
1186 (dip)	1188	1187	0.004	2	13
1173	1247	1242	0.089	~0	61
1107	1119	1118	0.011	11	20
1074	1079	1075	0.004	21	12
1051	1056	1060	0.003	15	11
1001	1012	1011	0.007	19	15
943	953	–	0.008	16	16
758	777	776	0.031	15	28

a) observed frequency, b) unperturbed frequency, c) unperturbed frequency observed in Raman spectrum, d) dimensionless coupling constant, d) linewidth, f) emv coupling constant defined by $(\lambda_\alpha\omega_\alpha/\chi(0))^{1/2}$.

The emv coupling constant g_α, which is defined by $g_\alpha = (\lambda_\alpha\omega_\alpha/\chi(0))^{1/2}$ and independent of the position and intensity of the charge-transfer band, is given in the last column of Table 3. The most strongly coupled mode is the 1173 cm^{-1} band, the

unperturbed frequency of which is 1247 cm^{-1}. In the case of TTF, ν_3 mode (1420 cm^{-1}), which is assigned to the symmetric stretching of the central and ring C=C bonds, couples most strongly with a charge-transfer state. Although BDNT has a fulvalene-like skeleton, the vibrational mode involving the C=C stretching, which corresponds to the 1462 cm^{-1} band, is significantly weaker than the strongest one. The strongest vibrational mode involves the stretching of the naphthothiadiazole ring of BDNT. The medium coupling of C=C stretching will be understood by the S···N attractive force, which fasten the dithiole ring with naphthothiadiazole ring and makes this molecule rather rigid.

When a charge goes out or comes in, the molecule relaxes into the most appropriate geometry. This relaxation energy gained by a small geometrical change of the molecule is expressed by the small polaron binding energy $\sum_\alpha g_\alpha^2 / \hbar\omega_\alpha$, which comes from the total geometrical change $\sum_\alpha \Delta q_\alpha = \sum_\alpha (2g_\alpha / \hbar\omega_\alpha)$. The corresponding energy of BDNT is 57 meV, which might be somewhat underestimated because our spectral range is limited down to 750 cm^{-1}. Two weak vibronic modes were found at 450 cm^{-1} and 510 cm^{-1} in the low-temperature powder spectrum. The binding energy therefore is estimated to be *ca.* 60-80 meV. This value is smaller than those of other molecules: 85 meV of $TCNQ^{-0.5}$ in MEM-$(TCNQ)_2$ [22], 99-136 meV of $TCNQ^{-1}$ in K-TCNQ[20], 88-127 meV of $TTF^{+0.2}$ in TTF-CA[21], and 242-308 meV of Chloranil ($CA^{-0.2}$) in TTF-CA[21]. This small relaxation energy means that the geometrical change accompanying the small charge oscillation around $BDNT^{+}$ ($1\pm\delta$) is smaller than those of TCNQ, TTF, or CA, in other words, $BDNT^{1+}$ is rather rigid. All these results are in accord with the geometrical consideration of $BDNT^{1+}$.

Possibility of a negative-*U* state

From the viewpoint of a molecular design, there seems to be two ways to look for negative-*U* materials. One way is to look for the molecules which shows one-step two-electron oxidation without a severe molecular deformation. Another way is to search for a molecule the geometry of which is planar in neutral and dicationic (or dianionic) states but non-planar in monocationic (or monoanionic) state. In the latter molecule, the

first oxidation potential will be pushed up and approaches to the second oxidation potential in solid state.

ACKNOWLEDGMENT

We are indebted to Dr. K. Imaeda of IMS for his assistance of the temperature-dependent resistivity measurement. We acknowledge Dr. M. Tomura of IMS for his assistance of the crystal structure analysis of BDNT-$(ClO_4)_2$-CH_2Cl_2.

REFERENCES

1 Y. Yamashita, K. Ono, S. Tanaka, K. Imaeda, and H. Inokuchi, Adv. Matter., 1994, 295.
2 The S···N distances are 2.776 Å in neutral BDNT, 2.652 Å in PF_6 salt, and 2.667 Å in ClO_4 salt, which are much shorter than the van der Waals contact (3.35 Å).
3 J. Dong, K. Yakushi, and Y. Yamashita, J. Mater. Chem., 5, 1735 (1995).
4 R. Micnas and J. Ranninger, Rev. Mod. Phys., 62, 113 (1990).
5 V. N. Denisov, A. N. Ivlev, B. N. Mavrin, K. Yakushi, J. Dong, and Y. Yamashita, Chem. Phys. Lett., 246, 176 (1995).
6 H. Kobayashi, A. Kobayashi, *et al.*, Bull. Chem. Soc. Jpn., 59, 301 (1986).
7 M. E. Kozlov, *et al.*, Spectrochim. Acta. Part A, 43, 323 (1987).
8 W. F. Cooper, *et al.*, J. Chem. Soc., Chem. Commun., 1971, 889.
9 R. Bozio, I. Zanon, A. Girlando, and C. Pecile, J. Chem. Phys., 71, 2282 (1979).
10 K. A. Abboud, *et al.*, J. Chem. Soc., Chem. Commun. 1993, 1560.
11 M. E. Kozlov, *et al.*, Spectrochim. Acta. Part A, 45, 437 (1989).
12 K. Yakushi, *et al.*, Acta Crystallogr., Sect. B, 36, 358 (1980).
13 A. Mursurkin and A. A. Ovchinniov, Soviet Phys. Solid State, 12, 2031 (1971).
14 D. Baeriswyl, J. Carmelo, A. Luther, Phys. Rev. B, 33, 7247 (1986).
15 K. Yakushi, T. Ida, A. Ugawa, H. Yamakado, H. Ishii, and H. Kuroda, J. Phys. Chem., 95, 7636 (1991).
16 M. Yoshitake, K. Yakushi, and H. Kuroda, unpublished data.
17 A. Ugawa, Thesis, the University of Tokyo p.135 (1989).
18 H. Tajima et al., Synthetic Metals 71, 1951 (1995).
19 Y. Tokura, Y. Kaneko, H. Okamoto, S. Tanuma, T. Koda, T. Mitani, and G. Saito, Mol. Cryst. Liq. Cryst., 12, 199 (1985).
20 M. J. Rice, N. O. Lipari, and S. Strassler, Phys. Rev. Lett., 39, 1359 (1977).
21 A. Painelli and A. Girlando, J. Chem. Phys., 84, 5655 (1986).
22 M. J. Rice, V. M. Yartsev, and C. S. Jacobsen, Phys. Rev. B, 21, 3437 (1980).